

## Seismic stability evaluation verification of slopes reinforced with prevention piles

H. Kobayakawa, M. Ishimaru, K. Hidaka A. Sekiguchi & T. Okada  
 Central Research Institute of Electric Power Industry, Japan

S. Mori  
 NEWJEC, Incorporated, Japan

K. Hiraga  
 Civil Engineering Research & Environmental Studies, Incorporated, Japan

H. Morozumi  
 Kansai Electric Power Company, Incorporated, Japan

**ABSTRACT:** In order to verify the stability evaluation flow of slopes with prevention piles installed, a model test of a slope was conducted. Prevention piles were designed to be installed on a slope with a distribution of successive weak layers, ensuring the safety factor of 1.2 for the design maximum seismic coefficient ( $K_H$ ) equal to 0.6, based on past stability evaluation flows. A slope model installed with prevention piles based on the design was created and a dynamic centrifugal force model experiment was conducted. As a result, it was confirmed that the prevention piles functioned even when the maximum horizontal acceleration ( $6.31 \text{ m/s}^2$ ) equivalent to the designed seismic coefficient worked, and that no noticeable change occurred on the slope. Based on these facts, the validity of the existing stability evaluation flow was demonstrated.

### 1 INTRODUCTION

In order to improve the seismic resistance of slopes around important structures, countermeasure construction is sometimes carried out (Nuclear Standards Committee of JEA 2016). The use of prevention piles is one effective measure. An earthquake stability evaluation method has been proposed for slopes with prevention piles (Toda et al. 2013). However, the effectiveness of the flow of stability evaluation has not been sufficiently verified, since it is difficult to ascertain the behavior of the actual slopes with the prevention piles installed at the time of the collapse. In order to verify the flow, a dynamic centrifugal model experiment was carried out on a model slope reinforced with prevention piles (Kobayakawa et al. 2017). In this paper, the effectiveness of the proposed stability evaluation flow is demonstrated from the results of the dynamic centrifugal model experiment.

### 2 PREVENTION PILE DESIGN BASED ON THE STABILITY EVALUATION FLOW

#### 2.1 The outline of the flow

The proposed flow is shown in Figure 1. Prevention piles for landslides are usually designed according to the guidelines for the steel pipe pile for landslide (Board of directors of the guidelines for the steel pipe

pile for landslide 2013). In this guideline, the concept of design differs depending on the pile deterrence mechanism. However, since the stress state of the piles and the surrounding ground during the earthquake is complicated, it is difficult to presume the deterrence mechanism in advance. Therefore, in this flow, the specifications of the prevention piles were decided based on the section force of the piles and the destruction state of the surrounding ground by a

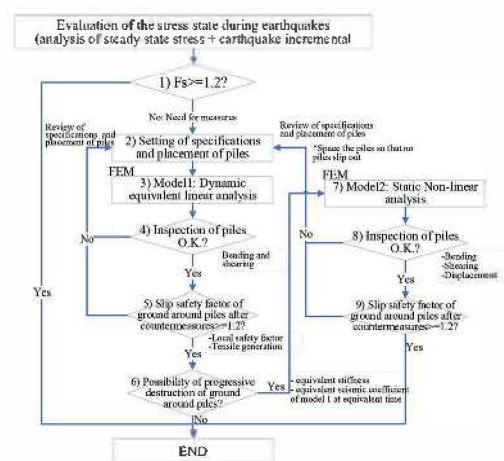


Figure 1. Flow of the seismic stability evaluation for slopes reinforced with prevention piles (Toda et al. 2013).

parameter study of dynamic equivalent linear analysis. Specifically, the section force of the piles was set so as to be within the elastic limit. With respect to the destruction of the ground around the piles, we checked the slip safety ratio of the ground surrounding the piles and determined the setting of the piles so as to secure an allowable safety factor of 1.2.

## 2.2 The model slope and pile design

### 2.2.1 Outline of the model slope

The cross-section diagram of the target slope is shown in Figure 2. The slope is a model used for centrifuge shaking tests. Since the size of the model slope used for the experiment was on a scale of 1 to 50, and the apparent gravity of the centrifugal acceleration set at 50G, the real scale of the height of the slope was 10m. The materials used for the slope consists of artificial soft rock and discontinuous plane, simulating a weak layer. The soft rock was compounded as shown in Table 1 in consideration of the homogeneity and strength of the material. The rock was left to sit for one week. The properties of the rock are as follows: The wet density ( $\rho_w$ ) = 2.07 Mg/m<sup>3</sup>, the initial shear modulus of rigidity ( $G_0$ ) = 933MPa, tensile strength ( $\sigma_t$ ) = 41.4kPa and the peak parameter for cohesion ( $c$ ) = 267kPa and the angle of shear resistance ( $\phi$ ) = 34.7° and. A Teflon sheet (thickness: 0.2mm) was used for the weak layer, in consideration of the ease of making a model and the reproducibility of physical properties. The mechanical properties of the weak layer are  $\rho_t$  = 2.10 Mg/m<sup>3</sup>,  $c$  = 0,  $\phi$  = 28.6° (at peak) and 19.3° (at residual).

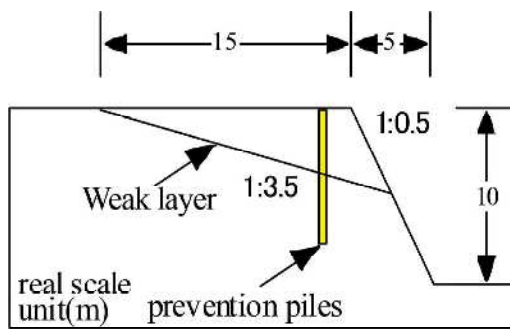


Figure 2. Shape of the slope

Table 1. Compound of the artificial soft rock.

Material	composition (kg/m <sup>3</sup> )
Cement	82
Crushed sand	817
micronized powder	817
admixture	1
Water	370

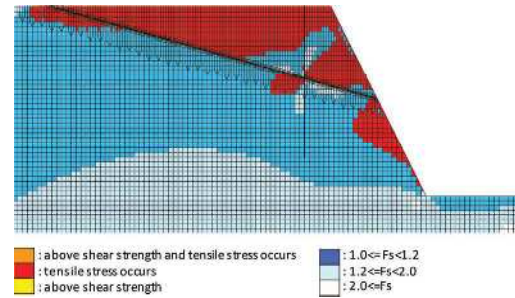


Figure 3. Distribution chart of local safety factor

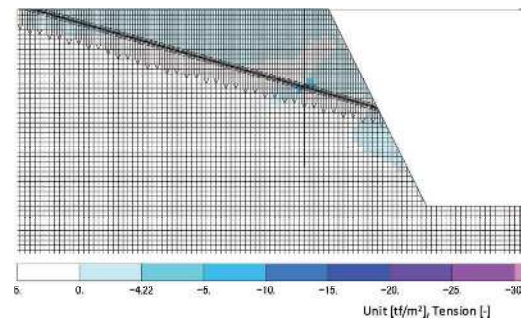


Figure 4. Distribution chart of tensile stress.

Based on these strengths, when the relationship between the slip safety factor and the horizontal seismic coefficient ( $K_H$ ) of the slope is calculated by the limit equilibrium method, the slip safety factor falls below 1.0 when  $K_H = 0.3$ .

### 2.2.2 The design of the piles

Based on the design philosophy of wedge piles and shear piles according to the guidelines for the steel pipe pile for landslide, the specification of prevention piles was determined so that the safety factor would be 1.2 or more for  $K_H = 0.6$  (Flow procedure 1)). As a result, on the real scale, the outer diameter of the piles was 0.4m, the thickness 15mm, the spacing between the piles 2m, the length 8m, and it was determined that the position of the piles would be set at 13.75m from the intersection of the slip surface and the ground surface (Flow procedure 2)).

Next, based on these specifications, an equivalent linear analysis was carried out on the slope model with the prevention piles. The cross-sectional force of the piles and the stress on the ground were calculated from the equivalent linear analysis, and the slip safety factor in front of the prevention piles and the possibility of progressive destruction were evaluated. The evaluation results are shown in Table 2. Procedures 3) and 4) of the flow meet the inspection reference value. An analysis of the local safety distribution diagram (Fig. 3) and the tensile stress distribution diagram (Fig. 4), however, shows that a stress exceeding

Table 2. Evaluation results of analyses.

Inspection items	Inspection result
Equivalent linear analysis	
Sectional force of prevention piles (allowable stress ratio < 1.0) (procedure 4))	Shear 0.13 < 1.0: O.K. Bending 0.038 < 1.0: O.K.
Slip safety factor in front of prevention piles (Fs > 1.2) (procedure 5))	Fs = 5.26 > 1.2: O.K.
Possibility of progressive destruction (procedure 6))	Possible occurrence of destruction in the weak layers (Fig.5). Tensile stress exceeding the tensile strength occurs around the prevention piles (Fig.6).
Static non-linear analysis	
Sectional force of prevention pile (allowable stress ratio < 1.0) (procedure 8))	Shear 0.27 < 1.0: O.K. Bending 0.116 < 1.0: O.K.
Slip safety factor in front of piles (Fs > 1.2) (procedure 9))	Fs = 2.59 > 1.2: O.K.

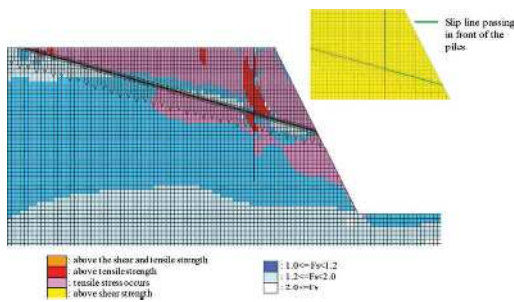


Figure 5. Distribution chart of local safety factor and failure element.

the tensile strength of the rock was generated at the intersection of the piles and the weak layers, which made it clear that there was a possibility of a progressive destruction.

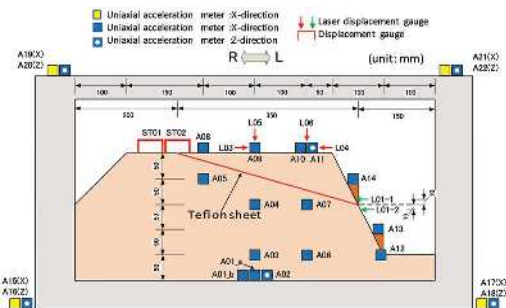
Therefore, a static non-linear analysis shown in the flow procedure 7) was conducted. The evaluation results are shown in Table 2, and the distribution of destruction elements and the local safety factor in the static non-linear analysis are shown in Figure 5. In the static non-linear analysis, there was a tendency for the tensile failure to progress towards the front of the prevention piles. Although the slip safety factor in front of the prevention piles became lower than that of the equivalent linear analysis, the section force and the slip safety factor of the piles satisfy the predetermined criteria. These results show that based on the flow shown in Figure 1, the specification of the piles installed on the slope was appropriately determined.

### 3 CENTRIFUGAL MODEL TEST OF THE SLOPE

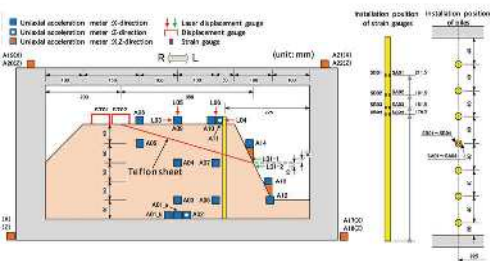
#### 3.1 Outline of the test

Stainless-steel pipes with an outer diameter of 8.0 mm and an inner diameter of 7.4 mm were used at the 1/50 scale of the piles studied in the design were used in the experiment. Seven piles were installed at intervals of 40 mm in the depth direction of the slope. The lower end of the model of the pile was fixed to the bottom of the soil tank, and strain gauges were attached to the inside of the prevention piles at the center of the model in the axial direction and the strain was measured.

The slope model and sensor placement are shown in Figure 6. Two types of experimental case were conducted: case 1 without prevention piles and case 2 with prevention piles installed. The slope height was 200 mm (10 m in real scale). The slope model was installed in a soil tank of 400 mm in length × 700 mm in width × 300 mm in depth, and two transparent silicone rubber sheets coated with petrolatum in between was placed between the side of the slope model and the wall of the soil tank to reduce friction. For the input acceleration waveform, a sinusoidal wave of 1.2 Hz at the actual conversion frequency was set to 20 waves in the main part, and four tapers were provided before and after the main part. The input acceleration was started at a small level, and a step shaking method was carried out in which the input level was incrementally increased after the shaking was completed at each step.



(1) Case1 (Unreinforced slope)



(2) Case2 (Slope reinforced with prevention piles)

Figure 6. Outline of the models

### 3.2 Result (case1)

The maximum horizontal acceleration ( $a_h$ ) and the visual observation results at each step are shown in Table 3. In shaking step d06 where the horizontal acceleration exceeds  $3 \text{ m/s}^2$ , it was confirmed for the first time that the rock mass at the upper part of the weak layers moved downward during the shaking. The residual displacement accumulated as the steps proceeded since the downward displacement remained after the end of the shaking at each step. The residual displacement after the shaking at each step are shown in Figure 7. In all the measurement results of the displacement, we can see how the rock mass from the upper part of the weak layers moves down the slope as the shaking step advances. The results of calculating the slip safety factor by the limit equilibrium method are also shown in Figure 7. The horizontal

Table 3. Maximum horizontal acceleration ( $a_h$ ) and observation at each step.

Step	$a_h \text{ m/s}^2$	Observation results
d01	0.30	d01~d05: No deformation confirmed visually.
d02	0.63	d06~d07: rock mass on the weak layer moves slightly downward along the weak layer.
d03	1.48	d08: rock mass on the weak layer moves 1 mm (at model scale) downward along the weak layer.
d04	2.01	d09: rock mass on the weak layer moves 1 mm (at model scale) downward along the weak layer.
d05	2.35	d10: rock mass on the weak layer moves 3 mm (at model scale) downward along the weak layer.
d06	3.02	
d07	3.09	
d08	3.50	
d09	3.92	
d10	4.27	

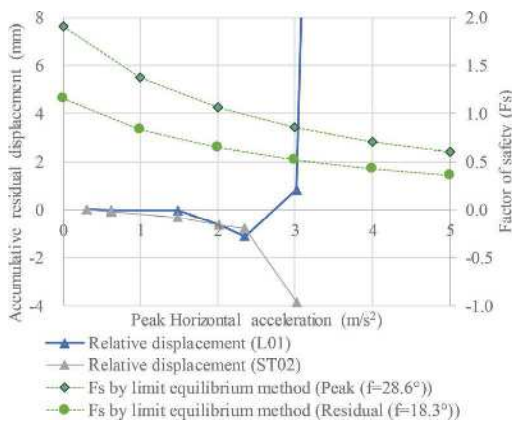


Figure 7. Residual displacement at each shaking step and slip Fs by limit equilibrium method.

acceleration (about  $3 \text{ m/s}^2$ ) where the slip safety factor by the limit equilibrium method was less than 1.0 and the horizontal acceleration of step d06 where the accumulative displacement was remarkably observed were almost in agreement.

### 3.3 Result (case2)

The maximum  $a_h$  and the visual observation results at each step are shown in Table 4. Although a shaking exceeding the input acceleration of the design was made for the first time in step d06, no deformation could be confirmed upon visual observation. The accumulative residual displacement captured by each displacement gauge are shown in Figure 8. In the displacement gauge ST02, the residual displacement transitioned at 1 mm or less until step d08, while about 50 mm of displacement occurred at step d09. In L01 at the front of the prevention piles, the residual displacement was 1 mm or less until step d08, as was the case with ST02, whereas displacement exceeding the measurement range of the sensor occurred at step d09.

## 4 EXAMINATION OF EXPERIMENTAL RESULTS AND VERIFICATION OF STABILITY EVALUATION FLOW

### 4.1 Verification of the design of piles based on the results of the equivalent linear analysis

As shown in Figure 1, in the stability evaluation flow of the pile design, the specification of the piles is first set based on the equivalent linear analysis. This is because it is considered that the behavior of the piles can be grasped by equivalent linear analysis in the range of design. Therefore, the validity of determining the specification of the piles based on the equivalent linear analysis is shown by comparing the experiment results of response of the piles and the surrounding ground with the analysis results.

Table 4. Maximum horizontal acceleration ( $a_h$ ) and observation at each step.

Step	$a_h \text{ m/s}^2$	Observation results
d01	0.72	d01~d08: No deformation confirmed visually.
d02	1.64	d09: rock mass above the weak layers vibrates back and forth after the shaking, then a crack will generate on the surface of the installation of the prevention piles. As the vibration continues, the crack propagates to the weak layer, and the rock mass at the front of the prevention piles is greatly displaced.
d03	2.65	
d04	3.42	
d05	4.76	
d06	6.31	
d07	8.64	
d08	9.32	
d09	11.47	

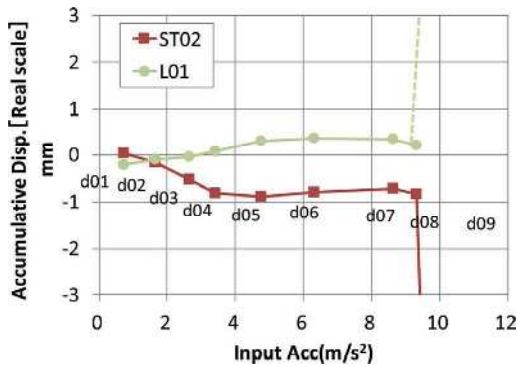


Figure 8. Relationship between input acceleration and accumulative displacement.

#### 4.1.1 Analysis condition

An analysis model diagram is shown in Figure 9. The slope ground was modeled by plane strain elements considering the non-linear characteristics of the material, and the weak layer part adopted a linear joint element. The prevention pile was modeled as a beam element and rigidly connected to the ground. The number of the piles was converted into the number per unit depth and then modeled. The boundary conditions were as follows: The bottom of the soil tank was completely constrained. A joint element was provided between the ground and the soil tank, and the value of the tangential spring of the joint element was set to 0, and the value of the vertical spring was set to be rigid so as to make it equivalent to the vertical roller. The properties of the soft rock and weak layer mentioned in 2.2 were used. The mechanical and physical properties of the prevention piles are shown in Table 5. For the input acceleration, the horizontal acceleration (A01-a) and the vertical acceleration (A02) measured at the bottom of the model were uniformly input to the bottom of the model. Input waves were given to every 20 seconds of each shaking step in the experiment.

#### 4.1.2 Analysis result and examination

The horizontal maximum acceleration for each step by experiment and analysis is shown in Figure 10.

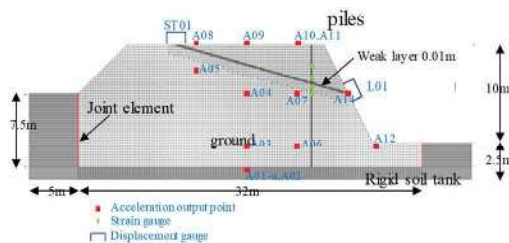


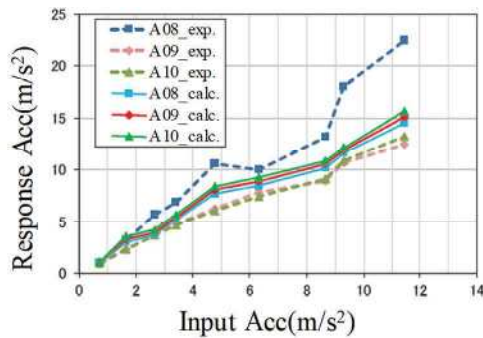
Figure 9. Analytical model. The model slope with a weak layer.

Table 5. Mechanical and physical properties of the prevention piles.

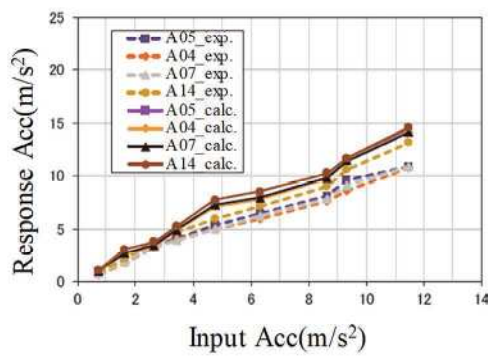
Properties	Per pile	Per unit depth
Shear modulus (GPa)	74.49	74.49
Poisson ratio	0.3	0.3
Sectional area (m <sup>2</sup> )	0.01814	$9.466 \times 10^{-3}$
Second moment of area (m <sup>4</sup> )	$3.367 \times 10^{-4}$	$1.571 \times 10^{-4}$
Unit weight (kN/m <sup>3</sup> )	77.8	36.3

The analysis results of the maximum horizontal acceleration distribution are almost consistent with the experimental value, except for measurement point A 08. The reason why the behavior of measurement point A 08 was different was that this measurement point was located in the immediate vicinity of the weak layer, and the upper rock mass of the weak layer was thinned, and it can be viewed that it may have been affected by the local behavior. In the acceleration time history, which will be described later, the peak acceleration of the measurement point is also larger than the other measurement points, but considering the behavior of the entire slope, it is thought to be a local behavior.

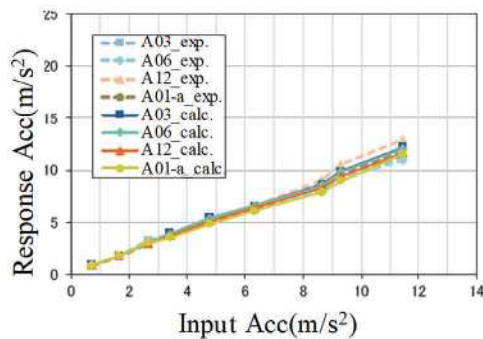
We focus on step d06 where the acceleration response value became the maximum within the range of design. As a representative example of the acceleration response at that step, the responses at A06, 07, 10, 11 around the piles are shown in Figure 11. The acceleration response values of the analysis results are either equal to or slightly larger than the experimental results, but have been calculated almost appropriately. In the range of design where displacement of the rock mass does not occur, the acceleration response has been appropriately evaluated. The time history of the axial force and the bending moment of the piles obtained from the measurement results of the strain gauge attached to the prevention piles is shown in Figure 12. The experimental and analytical values are generally consistent with respect to the section force of a piles in the rock mass above G.L. = 3.425 m near the weak layer. At the position of G.L. = 3.625 m, although the experimental and analytical values are consistent for the axial force, the bending moment is slightly larger in the analysis value. It is considered that the experimental value of the sectional force generated in the piles were smaller than the analysis value due to the local non-linearity of the surrounding ground where the piles and weak layer intersect. From the aspect of pile design, however, since the section force generated by the shake is estimated to be larger than the actual force, it is a setting on the side of prudence. For this reason, the evaluation is



(1) Top part of the model.



(2) Middle part of the model



(3) Bottom part of the model

Figure 10. Change in maximum acceleration at each shaking step.

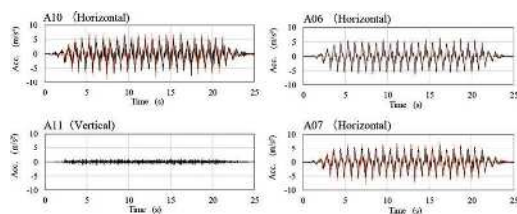


Figure 11. Time histories of the response acceleration (step d06)

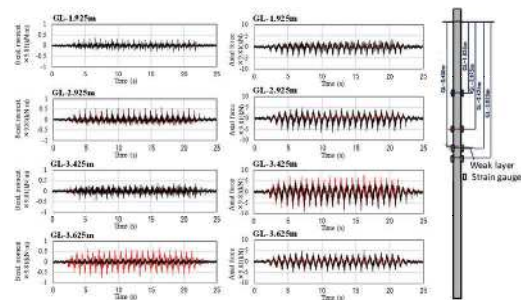


Figure 12. Time histories of the sectional force of pile (step d06).

appropriate as it becomes a setting on the safe side for piling design.

From the above results, it was confirmed that the response of the ground and piles obtained by the equivalent linear analysis is consistent with or slightly larger than the results of the experiment in the range of the horizontal seismic intensity set at the pile design. Therefore, it is considered that the design of the prevention piles based on the equivalent linear analysis is appropriate.

#### 4.2 The validity of the earthquake stability evaluation flow for slopes with prevention piles

A shaking experiment was carried out on the slope model created based on the specification of the prevention piles set by the flow shown on Figure 1. In the shaking step d06 (maximum  $a_h = 6.31 \text{ m/s}^2$ ) equal to or greater than the design seismic coefficient  $K_H = 0.6$ , it was confirmed that both the slope and the prevention piles were healthy without significant change occurrences. From these facts, the validity of the flow was confirmed. Furthermore, no noticeable variations such as slip or local failure of the slope were observed up to shaking step d08 (maximum  $a_h = 9.32 \text{ m/s}^2$ ) about 1.5 times the design seismic coefficient, and at shaking step d09 (maximum  $a_h = 11.47 \text{ m/s}^2$ ), about 1.8 times the design seismic coefficient, the rock mass at the front of the prevention piles collapsed (Table 4). This result shows that there is some allowance in the evaluation by this flow.

## 5 CONCLUSION

In order to investigate the validity of the stability evaluation flow of a slope on which prevention piles were installed, shaking tests were conducted in the centrifugal force field of the slope model with a weak layer. Based on the flow, the specification of the piles was determined so as to secure a slip safety factor of 1.2 or more against  $K_H = 0.6$ , and the piles were installed on a slope with a weak layer.

The shaking tests of the model slope confirmed that no noticeable change could be observed in either the prevention piles or the slope at the assumed input ground motion level. Based on these facts, the validity of the flow was demonstrated. For future earthquake risk assessment, it is necessary to establish a non-linear time-history analysis that can evaluate the behavior of the ground and piles in the range beyond the design input earthquake ground motions.

#### ACKNOWLEDGMENTS

This paper is the result obtained by the common research on nuclear risk center (FY2016) by 9 electric power companies, the Japan Atomic Power Company, Electric Power Development Co., Ltd. and Japan Nuclear Fuel Ltd.

#### REFERENCES

- Board of directors of the guidelines for the steel pipe pile for landslide. 2013. The guidelines for the steel pipe pile for landslide, Association for slope disaster management, 215pp (in Japanese).
- H. Kobayakawa, M. Ishimaru, A. Sekiguchi, T. Okada, T. Taniguchi, T. Hiraga, S. Mori and H. Nakamura. 2017. Earthquake stability evaluation of slope with prevention pile (part 1) - dynamic centrifugal force model experiment on prevention pile slope model -, *Japan Society of Civil Engineers 2017 Annual Meeting, Japan Society of Civil Engineering*, VII-20, pp.30–31 (in Japanese).
- Nuclear standards committee of JEA. 2016. Technical Guidelines for seismic design nuclear power plants. (JEAG4601-2015), The Japan electric association (in Japanese).
- T. Toda, H. Kobayakawa and K. Haraguchi. 2013. Dynamic stability of the rock slopes with prevention piles, *Abstract of the 52th annual meeting of the Japan landslide society, The Japan Landslide Society*, pp.126–127 (in Japanese).